

Shear-moment interaction of earthquake resistance confined masonry walls



15 WCEE
LISBOA 2012

J.J. Perez-Gavilan

Instituto de Ingeniería, Universidad Nacional Autónoma de México (UNAM)

A. Manzano

PhD. Student, Instituto de Ingeniería de la UNAM

SUMMARY:

Using as a *priory* hypothesis that drift is the main cause of first diagonal cracks due to tension, a prediction of a reduced shear force that cause cracking on earthquake resistance confined masonry walls is proposed as a function of flexural moment on its top. The reduction is relative to the nominal cracking shear force when no flexural moment is present on top of the wall. To verify the developed theory, a pilot study was conducted in which two full scale confined masonry walls were tested. The first wall subjected to cyclic lateral loads only and the second using cyclic loads, now including shear force and flexural moment. A reduction of the cracking shear force was observed in the second wall as expected and in good agreement with the prediction. Other observed differences are also described.

Keywords: Confined masonry, interaction, shear strength, flexure, cracking

1. INTRODUCTION

Confined masonry is extensively used in many countries in Latin America, including México, Peru, Chile etc., the Middle East, East Europe and south Asia (Riahi, Elwood and Alcocer, 2009). One of the main characteristics of the system is its sequence of construction. The wall is built first, with masonry units joined with mortar in running bond pattern. Once the wall is constructed small reinforced concrete tie-columns and tie-beams are cast in place to confine the wall. To increase its shear strength, horizontal reinforcement may be embedded in the mortar joints and anchored in the tie-columns (Hernández and Meli, 1976). For a complete description and practice refer to (Confined Masonry Network, 2011).

Extensive test have demonstrated that when built and detail adequately the walls may have adequate levels of displacement capacity and of shear, flexural and axial resistance. (Alcocer and Meli, 1995). Up to date this structural system is used for relatively low rise buildings: in México up to five floors and in other countries is restricted to one or two floor houses (NSR-10, 2010), (NZS, 2004). Accordingly, experiments have been conducted mainly with walls subjected to different levels of axial and a lateral loads with no direct application of flexural moment on top of the wall, as in low rise buildings its magnitude and effect is considered small compared to shear.

Influence of flexural moment has been associated to slenderness of the wall using the shear span ratio as parameter M/VL which can be interpreted as an effective aspect ratio H_e/L with $H_e = M/V$. Several authors (Meli, 1975),(Alvarez, 1996),(Zeballos et al., 1992), (Voon and Ingham, 2006) have referred to the effect of aspect ratio in shear strength. An increase in shear strength for decreasing aspect ratio is generally accepted for $M/VL < 1$. Let $M = VH + M_a$ where M_a is a flexural moment on top of the wall and H is the wall height; for slender walls $H/L > 1$ to have $M/VL < 1$ they must have a moment M_a on top of the wall in opposite direction to the moment produced by the shear force ($M_a < 0$). This moment produce a rotational restrain on top of wall. The presence of M_a can be seen as a reduction of the aspect ratio: $H_e = H/L - M_a/VL$. For squat walls, strength increases

proportionally with decreasing M/VL . In this case M_a may be positive or negative and still have $M/VL < 1$. As before the moment may be seen to increase or decrease respectively the aspect ratio of the wall. The effect of the flexural moment M_a is interpreted as a change in aspect ratio. No description of the effect of the flexural moment is included in codes for slender walls ($H/L > 1$ and $M_a > 0$) (MSJC SD, 2002), (NZS, 2004), (UBC SD, 1997), (CSA, 2004); an exception found in Peru's code (E.070, 2006).

Flexural moment may eventually produce tension in the wall, reducing the effective area to resist sliding shear as recognized by the Eurocode (EC6, 2002), however sliding shear strength is usually larger than diagonal tension shear strength (Tomazevic, 2009).

The contention in this paper is that the additional lateral deformation due to flexural moment affects the magnitude of the diagonal-tension cracking-shear-load and that the effects of aspect ratio and flexural moment need to be considered as independent variables for the prediction of shear cracking strength. Our first objective is to show the existence of shear-flexure interaction. Relating distortion with cracking an algebraic expression was deduced using elastic theory to predict the shear cracking strength, as a function of the basic masonry shear strength, related to the tensile strength of masonry, axial stress, aspect ratio and the flexural moment on top of the wall. Two full scale confined masonry walls were tested: the one used as reference, with a fixed axial force and increasing cycles of shear force, the second wall was similarly tested but now with an additional flexural moment on top of the wall. The results show that the flexural moment reduced the shear load that produced the first diagonal cracks and the reduction is in good agreement with the predictions.

2. HYPOTHESIS

The hypothesis states that cracking is due to the relative lateral deformation of the wall, disregarding which load produced such deformation: shear or a combination of shear and moment. A linear elastic behaviour of the wall is assumed as no predictions will be given after the first diagonal cracks appear in the wall. A shear displacement model of confined masonry is shown in Fig. 2.1 (Flores and Alcocer, 1996). Hereafter V_n will be used to refer to the cracking shear load when no additional moment is considered on top of the wall, and V'_n to the same value after considering the effect of the moment.

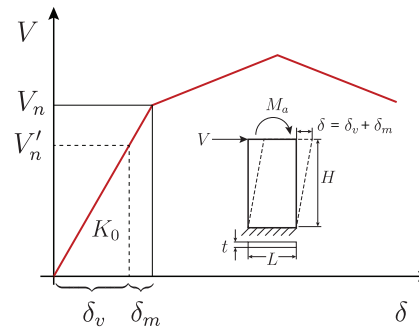


Figure 2.1 Model of shear –displacement envelope with K_0 as the wall stiffness, δ_v , δ_m the displacements due to shear force V and a flexural moment M_a , respectively.

Using a linear relationship between displacement and shear and elastic theory to calculate lateral displacements due to shear load and flexural moment the following formulas can be written

$$V'_n = V_n - \delta_m K_0 = V_n - \frac{M_a}{H_k}, \quad H_k = \frac{2k_f + k_v}{3} H \quad (2.1)$$

where

$$\delta_m = \frac{M_a H^2}{2EI}, \quad K_0 = \frac{k_f k_v}{k_f + k_v}, \quad k_f = \frac{3EI}{H^3}, \quad k_v = \frac{GA}{\kappa H}, \quad I = \frac{tL^3}{12}, \quad A = tL \quad (2.2)$$

E , G are masonry modulus of elasticity and shear modulus respectively, κ the shear factor and L , H are the total length and height of the wall. Using normalized parameters, $w = H/L$, $M_a = \beta V_n' H/2$ and $\eta = G/E$, the quotient of the cracking shear force considering and without considering the effect of a flexural moment M_a on top of the wall $\alpha = V_n'/V_n$ may be written as

$$\alpha = \frac{1}{1 + \frac{15\beta\eta w^2}{20\eta w^2 + 6}} \quad (2.3)$$

Parameter β is convenient as it represents the amount of flexural moment, and depending on its value, several conditions may be readily identified: if $\beta = -1$ the wall has its upper end rotationally restrained, if $\beta = 0$ the wall is in cantilever and otherwise the wall undergoes a fixed rotation of its top, larger than that of a cantilever. In Fig. 2.2.a α is plotted as a function of aspect ratio for different values of the moment parameter β and two values of η . No effect on cracking strength is predicted for very long walls ($\alpha = 1$), as lateral displacement due to flexure is very small, but it rapidly decreases as the wall gets shorter getting asymptotic to $V_n' = V_n \cdot 4/(4 + 3\beta)$. In Fig. 2.2.b α is plotted as a function of β in this case for different values of aspect ratio. As it should, there is no effect if there is no moment applied ($\alpha = 1, \beta = 0$), and when it is applied in the opposite direction to the moment generated by the shear force ($\beta < 0$) an increase on cracking strength is predicted ($\alpha > 1$). Meli, (Meli, 1975) described this effect in terms of aspect ratio for tests conducted restraining the rotation of the top of the wall, tests known as diagonal compression tests; here the effect of moment and aspect ratio are clearly separated. In the cases plotted, the effect increases with parameter $\eta = G/E$. This prediction should be expected as when η increases shear deformation is reduced i.e. increasing the ratio of flexural to shear deformation; consequently the effect of moment is more pronounced.

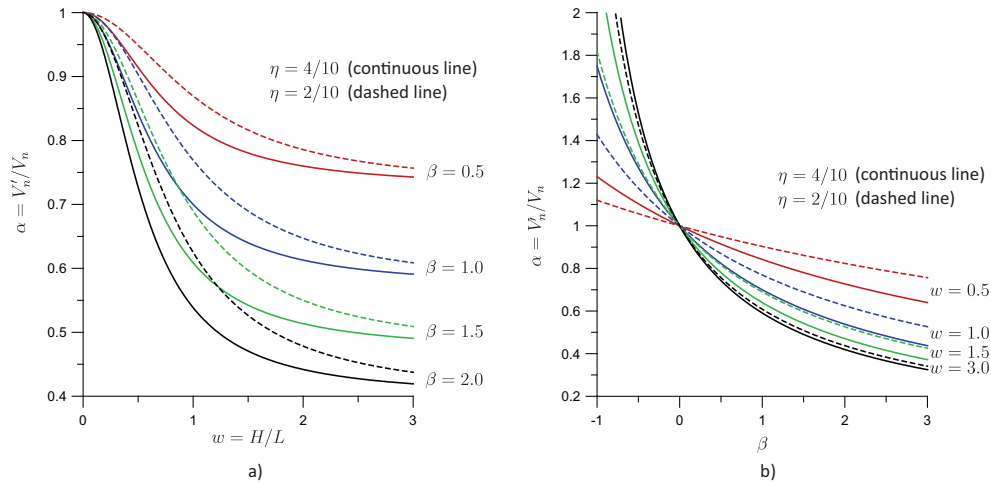


Figure 2.1 a) V_n'/V_n as a function of aspect ratio w , b) V_n'/V_n as a function of the applied moment parameter β

3. EXPERIMENTAL PROGRAM

3.1. Specimens

Two full scale confined masonry walls specimens M1 and M2 were built. Solid clay masonry units $23.4 \times 11.8 \times 5.3$ cm were used, joined with mortar 1:3 cement to sand ratio in running bond pattern. Tie column section was 11.8×15 cm reinforced with four 9.5 mm diameter steel bars ($f_y = 412$ MPa) and stirrups every 18 cm made of 6.35 mm diameter bars ($f_y = 248$ MPa). Tie beams section was 11.8×16 cm reinforced as the tie columns. (see Fig. 3.1). Average masonry compression strength f_m and average shear strength v_m were obtained with standard ASTM tests, along the masonry modulus of elasticity E_m and shear modulus G_m respectively. Similarly the concrete compression strength f_c' and

corresponding modulus of elasticity E_m were obtained, see Table 3.1.

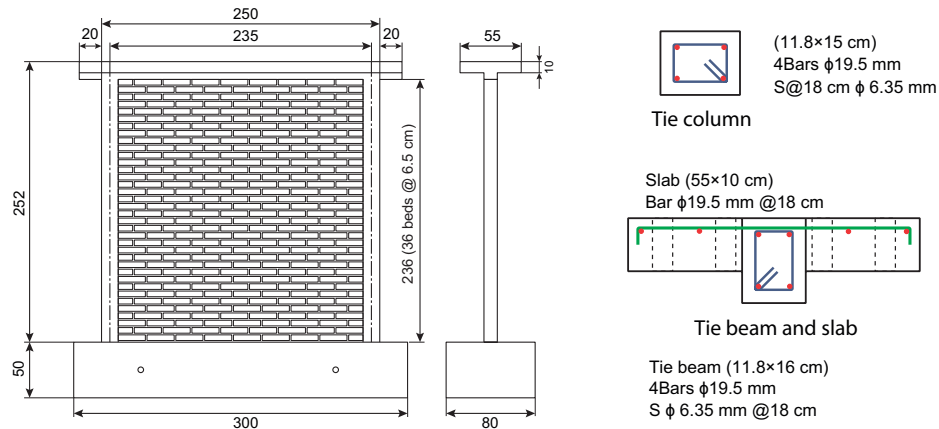


Figure 3.1 Specimen dimensions and reinforcement

Table 3.1 Material properties

	f_m (MPa)	v_m (MPa)	E_m (MPa)	G_m (MPa)	f'_c (MPa)	E_c (MPa)	f_y (MPa)	E_s (MPa)
M1	4.45	0.31	623.11	171.52	23.24	10352.68	404.13	205998
M2	4.53	0.33	785.51	139.65	21.28	8088.33	404.13	205998

3.2. Setup

The laboratory setup used to apply lateral load, vertical load and moment is depicted in Fig. 3.2. A steel beam was put on top of the wall and fastened to the slab with 22.2 mm diameter bolts arranged symmetrically relative to the plane of the wall, to distribute the horizontal load uniformly along the wall top, to simulate the inertia forces distributed by a building floor slab in an earthquake. Vertical actuators were used to apply the vertical and flexural loads.

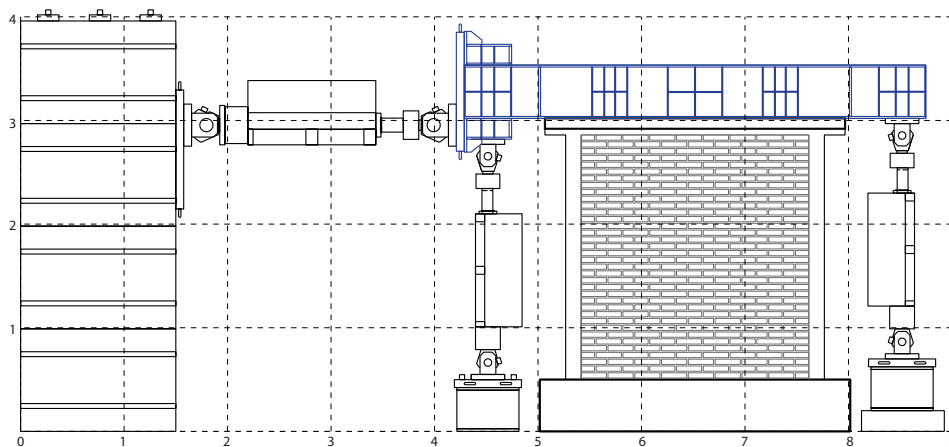


Figure 3.2 Experimental setup

3.3. Load sequence

Both specimens were subjected to a vertical load $P = 392$ kN ($\sigma = 1.32$ MPa). For the reference wall M1 no moment on top of the wall was included. The vertical load was applied first followed by two load controlled cycles of shear load up to $0.25 V_n$ and two more cycles that reached $0.5 V_n$, being V_n the nominal shear load that produce the first diagonal cracks in the wall, according to the Mexican

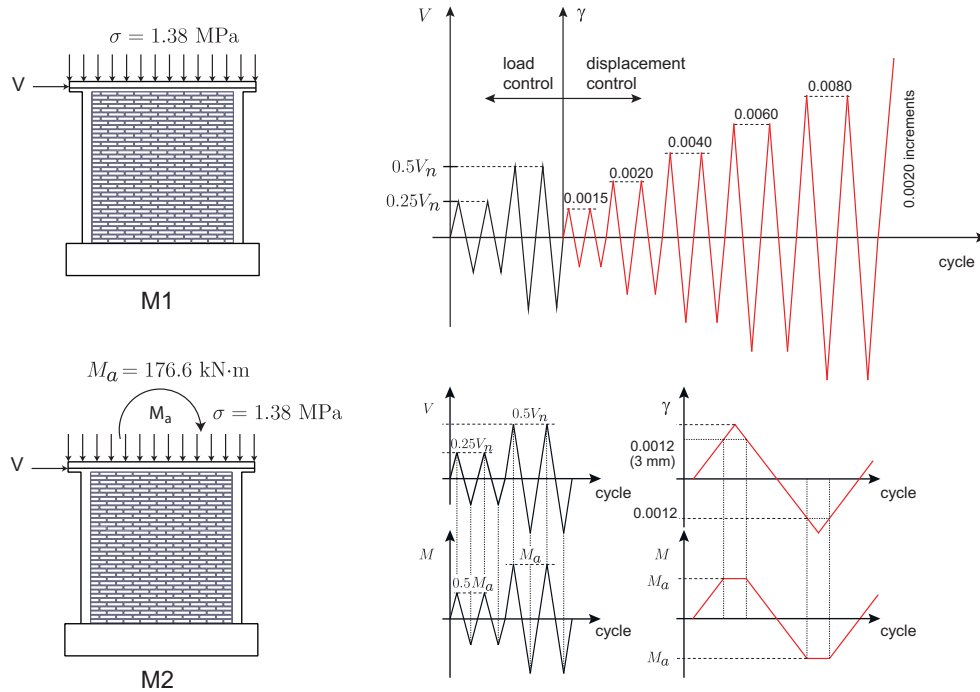


Figure 3.3 Load sequence

code (NTCM, 2004):

$$V_n = 0.5v_m A_T + 0.3P \leq 1.5v_m A_T \quad (3.1)$$

Afterwards the sequence changed to displacement control, applying pairs of cycles with increasing deformation $\gamma = \delta/H = 0.0015, 0.002, 0.004, 0.006, 0.008, \dots$ etc. The test stopped when a crack completely crossed one of the tie columns; event that coincided with failure. The load sequence for wall M2 was entirely similar to the one used for M1 with respect to the lateral load and lateral displacements; additionally a moment was applied. During the load control sequence, cycles with one repetition each were applied reaching $(0.25V_n, 0.5M_a)$ and $(0.5V_n, M_a)$. For the displacement controlled cycles a moment was applied linearly increasing with displacement up to M_a when the lateral deformation reached 0.0012 (3 mm). Similarly when unloading, moment M_a was maintained until the value of deformation came down to 0.0012, when it started to decrease linearly with deformation towards the negative branch of the cycle. The intention was to assure that the desired level of moment was attained before the first diagonal cracks appear due to shear. (See Fig. 3.3)

4. RESULTS

Hysteresis curves are shown in Fig. 4.1. For Wall M2 the two parallel dashed lines mark the deformation ± 0.0012 used to stop/start the variation of moment as explained in the load sequence section. Table 4.1 reports the shear and lateral displacements that were logged when the first diagonal cracks appeared, at peak shear strength and ultimate strength, for the positive and negative branches of the hysteresis curve. Ultimate strength was achieved when the lateral load decreased to $0.8 V_{max}$. Table 4.2 shows the deformations corresponding to the displacements in Table 4.1, of the positive branch, and the ductilities at shear strength and ultimate strength; it also reports the accumulated energy dissipated up to when the first inclined cracks appear in the wall.

4.1. Crack patterns

Final crack patterns are shown in Fig. 4.2. Both walls show inclined cracks due to shear with a similar

pattern; however, wall M2 exhibit a more distributed pattern and a greater number of smaller cracks. South tie column of wall M2 shows initiation of crushing of its cover attributed to the additional flexural moment.

Table 4.1. Shear force and lateral displacements at cracking, peak strength and ultimate strength

Wall	Cracking				Peak strength				Ultimate			
	V_c^+ (kN)	d_c^+ (mm)	V_c^- (kN)	d_c^- (mm)	V_{max}^+ (kN)	d_{max}^+ (mm)	V_{max}^- (kN)	d_{max}^- (mm)	V_u^+ (kN)	d_u^+ (mm)	V_u^- (kN)	d_u^- (mm)
M1	143.4	4.75	-151.1	-4.50	188.9	15.12	-151.1	-94.50	170.2	15.37	-111.0	-14.32
M2	110.5	4.97	-96.2	-4.94	176.4	19.62	-154.7	-14.72	176.4	19.62	-150.5	-14.76

Table 4.2 Deformations and ductilities

	γ_c	γ_{max}	γ_u	γ_{max}/γ_c	γ_u/γ_c	E_d kN·mm
M1	0.00193	0.00616	0.00626	3.19	3.24	900
M2	0.00203	0.00801	0.00801	3.95	3.95	752

E_d = Dissipated energy up to first inclined cracking

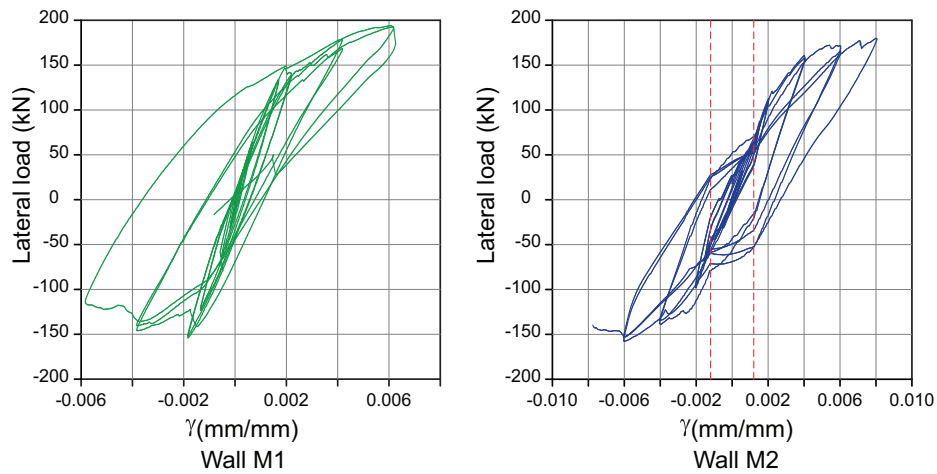


Figure 4.1 Hysteresis curves

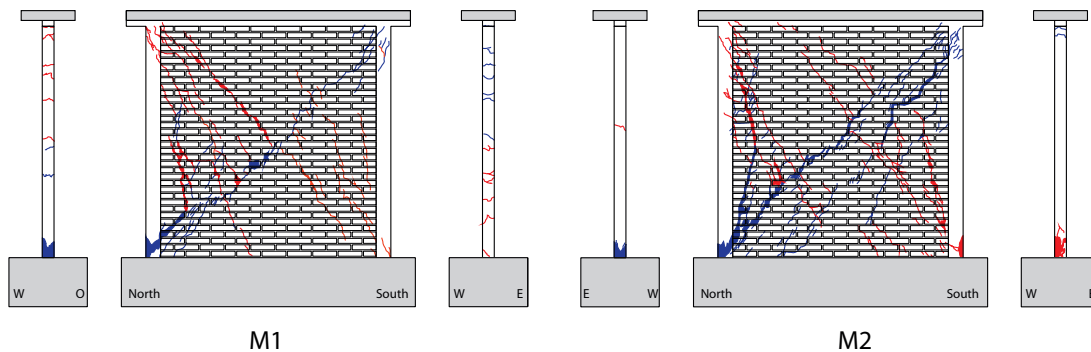


Figure 4.2 Final crack patterns

4.2 Envelopes

Envelopes of the hysteresis curves are presented in Fig 4.3. The stiffness of wall M2 is smaller than that of M1, as the lateral displacements of wall M2 are due to a shear force and a moment, so clearly

the same lateral displacement is reached with a smaller shear force. When the moment stopped to increase, as marked by the dashed line, there is a sudden stiffness increase; being then much similar to that of M1, as only the lateral load is changing. (See M2 curve from the dashed line towards 110.5 kN in the positive branch and towards -96.21 in the negative branch). In both the positive and negative branches of M2 cracking occur after M_a was attained as required. (i.e after the dashed line). Cracking shear load is reduced for M2 as expected; a comparison to the predicted value is done later. The shear strength was also reduced; however the prediction of this reduction is outside the scope of the used theory.

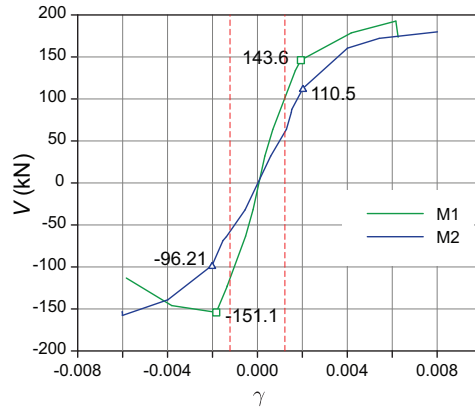


Figure 4.3 Envelopes of hysteresis curves

4.3 Stiffness degradation and energy dissipation

Cycle stiffness was used to track the changes on stiffness with lateral deformation. Cycle stiffness and average deformation is defined for each loop of the hysteresis curve as

$$K = \frac{V^+ - V^-}{\delta^+ - \delta^-} \quad \gamma = \frac{\delta^+ - \delta^-}{2H} \quad (4.1)$$

Where V^+ and V^- are the peak shear forces of the positive and negative branches of the loop; and δ^+ and δ^- are the corresponding peak displacements. Fig. 4.4.a shows the evolution of the cycle stiffness with average deformation. Wall M2 had slower stiffness degradation with lateral deformation,

$$E_d = \frac{\sum_{i=1}^n V_i (d_{i+1} - d_{i-1})}{2} \quad (4.2)$$

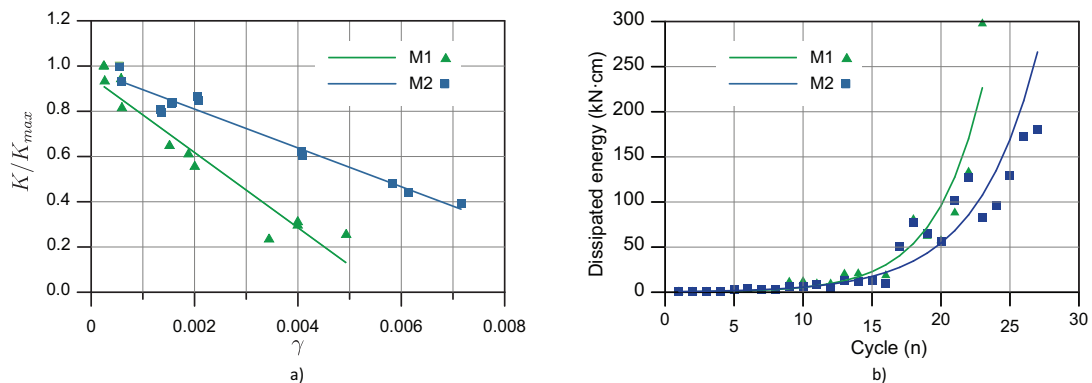


Figure 4.4. a) Stiffness degradation, b) Energy dissipation

presumably due to the fact that some of the lateral deformation was caused by flexure. An alternative measure of wall damage is the energy dissipated by cycle, that is where n is the number of sample points in the cycle, d_i, V_i are the displacement and shear force of sample point i . Fig. 4.4.b shows the energy dissipated by cycle for both walls. As with the case of stiffness degradation, in this case, M2 dissipated less energy, again attributed to the fact that the displacements were due, in greater amount, to flexure.

4.4 Shear and flexural deformations

The amount of flexural and shear deformation was also evaluated using as shear displacement

$$\gamma = \frac{L}{2H} \left(\frac{\Delta_1}{D_1} + \frac{\Delta_2}{D_2} \right) \quad \Delta_s = \gamma H \quad (4.3)$$

where Δ_1 and Δ_2 are the measured cycle's peak left and right diagonal displacements, D_1 and D_2 the measured lateral displacements measured in opposite sides of the wall. The rest of the measured lateral displacement was considered due to flexure, Fig. 4.5 shows the evolution of shear and flexural displacements by cycle.

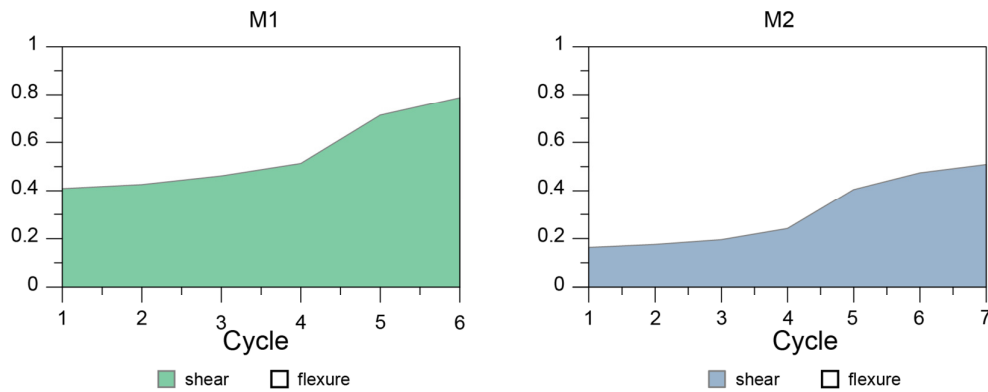


Figure 4.5 Shear and flexural deformation

The marked difference of flexural to shear deformation is well represented by the graphs. Shear deformation increases as soon as cracking initiates in the walls.

5. SHEAR-MOMENT INTERACTION

To evaluate $\alpha = V_n'/V_n$, the nominal cracking shear force was obtained from the cracking shear force of Wall M1 $V_n = 143.6$ kN, tested without moment, while $V_n' = 110.5$ kN was the cracking shear force of Wall M2, tested with a total moment equal to $M_a = 176.52$ kN-m; i.e. α (experimental) = 0.77. The predicted value is given by Eqn. (2.3); the aspect ratio was nearly equal to 1 ($w = 1$), the average

Table 5.1. Comparison of experimental and theoretical results

	M1	M2
M_a (kN-m)	0.0	176.5
P (kN)	392.3	392.3
V_n (kN)	143.6	143.6
V_n'		110.5
$\beta = M_a/(V_n'H/2)$	0	1.3
α (calculado)	1	0.71
α (experimental)	1	0.77

$\eta = G/E = 0.23$ was obtained from the material tests and $\beta = M_a/(V_n'H/2) = 1.3$, using the previous parameters the theoretical value of α (theory)=0.71. Table 5.1 presents a summary of the parameters and result. The relative error of the prediction was 7.8% $((0.71-0.77)/0.77 \times 100=7.79)$.

6. CONCLUSIONS

Based on the results of the tests and their comparison to the analytical predictions the following conclusions may be drawn:

- The presence of flexural moment on top of the wall affects the magnitude of the shear force that produces the first inclined cracks due to tension in a confined masonry wall: i.e. shear cracking strength is not independent from the level of flexural moment.
- The hypothesis in which the lateral deformation at cracking is the same whether it was caused by a lateral load or a lateral load and moment was satisfied to a reasonable level of accuracy only 4.6% deviation in the positive branch and 9.8% of deviation in the negative branch. However, because both walls initiate cracking in the positive branch, the former value is considered more representative, while the larger deviation in the negative branch, may be attributed, in part, to nonlinear effects, as some damage in the wall was present, not considered in the developed theory.
- The reduction in the shear force that produced diagonal tension cracks was estimated with good accuracy, with 7.8% deviation from experiment.
- Stiffness degradation and energy dissipation curves show that wall damage is less severe when the lateral displacements are due to flexure, as compared with the damage caused by lateral forces only.
- Ductilities defined herein as displacements at peak strength and ultimate strength divided by the displacement at cracking, which is also considered a limit of the elastic range, increased when displacements were produced by shear force and moment, as compared with those obtained with shear forces only (see Table 4.2).
- The presence of flexural moment in a wall should explicitly be considered to estimate the shear capacity of the wall. Although no predictions are made here for the shear strength of the wall, the experimental results presented here show that the shear strength is affected by the flexural moment.

7. FINAL REMARKS

The developed theory separates the effect of moment and slenderness by keeping both β and w : the amount of moment (boundary condition) and aspect ratio parameters, respectively, as independent variables. The effects those have been traditionally intertwined by using the shear span ratio or the effective height.

An ongoing investigation is being conducted to confirm the presented results for walls with different aspect ratio w and moment β .

An analytical study is required to investigate the range of β for different seismic conditions and number of floors of the structure. The results of such an investigation together with the given theory will give a complete map of the importance of the shear-moment interaction in confined masonry walls.

ACKNOWLEDGEMENT

The investigation was supported by the Federal District Government (GDF) grant No CT/04/10 and partially by the Science and Technology National Council (CONACYT) Grant No 133225. The tests were conducted at the

Structures Lab of the Institute of Engineering (UNAM) with Eddy Grandry† as control technician and support personnel of the Lab, Raymundo, Salomon, Ismael and Agustin.

REFERENCES

- Alcocer, S. and Meli, R. (1995) Test program on the seismic behaviour of confined masonry walls, *The Masonry Soc. J.* (Boulder), **12:2**, 68-76.
- Alvarez, J.J. (1996) Some Topics of the seismic behaviour of confined masonry structures, *Eleventh World Conference on Earthquake Engineering*.
- Confined Masonry Network (2011) Seismic Design Guide for Low-Rise Confined Masonry Buildings, World Housing Encyclopedia, EERO & IAEE.
- CSA (2004) S304.1-04 Design of Masonry Structures, Mississauga, Ontario, Canada: Canadian Standard Association.
- E.070 (2006) Norma Técnica E.070 Albañilería, Perú.
- EC6 (2002) Eurocode 6: Design of Masonry Structures --Part 1-1: Common rules for reinforced and unreinforced masonry Structures, European Standards.
- Flores, L.E. and Alcocer, S.M. (1996) Calculated response of confined masonry structures, *11th World Conf. on Earthquake Engineering*.
- Hernández, O. and Meli, R. (1976) Modalidades de refuerzo para mejorar el comportamiento sísmico de muros de mampostería No 382, México, D.F.: Instituto de Ingeniería, UNAM.
- Meli, R. (1975) Comportamiento sísmico de muros de mampostería No 352, México, D.F.: Instituto de Ingeniería, UNAM.
- MSJC SD (2002) TMS 402-08/ACI, 530-08/ASCE 6-08, Building Code Requirements and Specification for Masonry Structures, Masonry Standards Joint Committee.
- NSR-10 (2010) Reglamento Colombiano de Construcción Sismo Resistente, Bogotá D.C., Colombia: Ministerio de Ambiente, Vivienda y Desarrollo Territorial.
- NTCM (2004) Normas Técnicas Complementarias para diseño y construcción de estructuras de mampostería, Mexico: Gobierno del Distrito Federal (in Spanish).
- NZS (2004) (4230:2004) Design of Reinforced Concrete Masonry Structures, Wellington: Standards Association of New Zealand.
- Riahi, Z., Elwood, K.J. and Alcocer, S.M. (2009) Backbone Model for Confined Masonry Walls for Performance-Based Seismic Design, *Journal of Structural Engineering*, **135**,644-654.
- Tomazevic, M. (2009) Shear resistance of masonry walls and Eurocode 6: shear versus tensile strength of masonry, *Materials and Structures*, **42**, 889-907.
- UBC SD (1997) Uniform Building Code, Whittier, California: International Conference of Building Officials.
- Voon, K.C. and Ingham, J.M. (2006) Experimental In-Plane Shear Strength Investigation of Reinforced Concrete Masonry Walls, *Journal of Structural Engineering*, March, **132:3**,400-4008.
- Zeballos, A., San Bartolomé, A., Muñoz, A. and. (1992) Efectos de la esbeltez sobre la resistencia a fuerza cortante de los muros de albañilería confinada. Análisis por elementos finitos, *Blog de Angel San Bartolomé, Pontificia Universidad Católica de Perú*, <http://blog.pucp.edu.pe/media/688/20070504-Esbeltez%20-%20Elementos%20finitos.pdf>.